Eze et al., *Cogent Engineering* (2017), 4: 1339336
https://doi.org/10.1080/23311916.2017.1339336

cogent engineering

ELECTRICAL & ELECTRONIC ENGINEERING | RESEARCH ARTICLE

Maximum power point tracking technique based on optimized adaptive differential conductance

Val Hyginus U. Eze[1]*, Ogechukwu N. Iloanusi[1], Martin C. Eze[1] and Charles C. Osuagwu[1]

Received: 13 January 2017
Accepted: 29 May 2017
First Published: 15 June 2017

*Corresponding author: Val Hyginus U. Eze, Electronic Engineering, University of Nigeria, Nsukka, Nigeria
E-mail: ezehyginusudoka@gmail.com

Reviewing editor:
Qingsong Ai, Wuhan University of Technology, China

Additional information is available at the end of the article

Abstract: Maximum power point (MPP) tracking technique based an optimized adaptive differential conductance technique was developed in this paper. The performance of the algorithm developed in this paper was evaluated at solar irradiance of 1,000, 800 and 600 W/m^2 and at temperature of 298, 328 and 358 K. From the simulation results, it was observed that the impedance of the panel decreases as the irradiance increases while the impedance of the load is not affected by the irradiance. This technique was also validated with conventional incremental conductance (INC) technique. From the validation result, the resultant conductance of the optimized adaptive differential conductance technique at MPP is 0.0030 mho higher than resultant conductance at ideal condition while conventional technique has the resultant conductance of 0.0418 mho lower than the resultant conductance at ideal condition. From the analysis, the technique has a relative improvement of 6.0558% compared to the conventional INC technique. The simulation was done using Matrix Laboratory (MATLAB).

Subjects: Mathematics & Statistics; Computer Science; Engineering & Technology

Keywords: incremental conductance technique; maximum power point; maximum power point tracking; optimized adaptive differential conductance; photovoltaic

Val Hyginus U. Eze

ABOUT THE AUTHORS

Val Hyginus U. Eze obtained BE in the Department of Electrical/Electronic Engineering from Enugu State University of Science and Technology, Enugu and ME in Electronic Engineering from University of Nigeria, Nsukka (UNN). Currently, I am a PhD student in University of Nigeria, Nsukka.

Ogechukwu N. Iloanusi is a co-author and a Senior Lecturer at the Department of Electronic Engineering, UNN. She holds a PhD in Digital Electronics and Computer.

Martin C. Eze is a co-author and he holds his BE and ME in Electronic Engineering from UNN. Currently he is a PhD student in UNN.

Charles C. Osuagwu is a co-author and a professor of Electronic Engineering, in the UNN.

Our research areas include digital signal processing (DSP), Digital Systems Design and Photovoltaics. They all contributed so intensively both in algorithm development and in result analysis. This project will help in the PV design for accurate tracking.

PUBLIC INTEREST STATEMENT

This paper developed a mathematical expression (model or algorithm) that will ensure optimum transfer of generated power from solar panel to load when implemented in the charge controller. The model was developed using a single diode model. When implemented in charge controller, the model will perform the function of matching the panel impedance to the load impedance to ensure optimum power transfer to the load. The significance of this model is that it will lead to the implementation of better MPPT-based charge controller for photovoltaic application. Charge controller built using this model will maximize power transfer from PV panel to the load with minimal power loss. The maximum power is transferred to load when the panel conductance is equal to the load conductance and this occurs at maximum power point. The model is very fast and accurate in matching panel impedance and load impedance.

cogent oa

© 2017 The Author(s). This open access article is distributed under a Creative Commons Attribution (CC-BY) 4.0 license.

1. Introduction

In the past few years, solar energy is one of the most important renewable energy sources that have been gaining increased attention. The amount of energy supplied to the earth by the sun in a day is sufficient to power the total energy needs of the earth in a year (Azimi, Dehkordi, & Niroomand, 2012). A comparative study of the world energy consumption released by International Energy Agency shows that in 2050, more than 45% of necessary energy in the world will be solely produced by solar arrays.

The basic structural unit of a solar system is the PV module, which consists of solar cells (Safari & Mekhilef, 2011). A solar cell converts the energy in the photons of sunlight into electricity by means of the photovoltaic phenomenon found in the certain type of semiconductors such as silicon, germanium, and selenium.

Photovoltaic (PV) systems are rated in terms of maximum power which is the highest power that can be generated by PV system under Standard Test Condition (STC). The power output efficiency of the solar module depends on many factors such as temperature, irradiance and spectral characteristics of sunlight (Safari & Mekhilef, 2011). At STC the temperature is 25°C, solar irradiance is 1,000 W/m^2, air mass is 1.5, wind speed is 2 m/s and solar panels tilt angle when it faces south is 30° (Eze & Olisa, 2015; Topic, Brecl, Kurnik, & Sites, 2006). Under normal operating conditions, maximum power generation from PV is not possible because the PV panel cannot always be operating at optimum power. PV systems generate the highest amount of power when the incident sun beam is perpendicular to the panel. The effective utilization of power from the sun using PV systems is improved by adding PV Efficiency Enhancement (EE) systems. Examples of EE systems are the solar tracking system and maximum power point (MPP) tracking systems.

The solar tracking system was the conventional method used to align PV panel to the direction where the solar irradiation is highest. The main drawback of this technique was that the solar tracking system is so expensive, difficult to maintain and the power generated is not well utilized due to power losses during transfer (Nguyen, Low, & Member, 2010). Due to the drawbacks of solar tracking techniques, maximum power point tracking (MPPT) was introduced. For the power generated by the PV system to be utilized well, MPPT technique is developed to enhance the utilization of power generated by the PV. Not all the power generated by PV panel is transferred to the load.

PV modules transfer the highest percentage of power generated to the load at MPP. MPP is a point along the P-V characteristic of a PV panel where the photovoltaic impedance is equal to the load impedance. It is also a point where there is negligible energy loss in the transmission of the generated power to the load. MPP along the P-V curve is detected using MPPT techniques. MPPT is the method of operating the photovoltaic system in a manner that allows the modules to transfer most of the power generated to the load. It is implemented in charge controllers alongside battery charge level monitoring system. MPPT varies the electrical operating point of the PV system so that the module will deliver nearly all the generated power to the load. It ensures that maximum power is transferred from the photovoltaic (PV) panel to the load (Chafle & Vaidya, 2013).

An example of MPP technique is incremental conductance (INC) method. INC method makes use of instantaneous conductance (panel) and INC (load) to determine the MPP. Resultant conductance is determined by the instantaneous conductance $\left(\frac{I}{v}\right)$ and INC $\left(\frac{dI}{dv}\right)$ as shown in Equation (1). For an ideal INC, the resultant conductance (the slope of the P-V curve) at MPPT is zero as in (2). For a perfect condition to be achieved in MPPT based on INC technique, Equation (2) must be satisfied (Chafle & Vaidya, 2013).

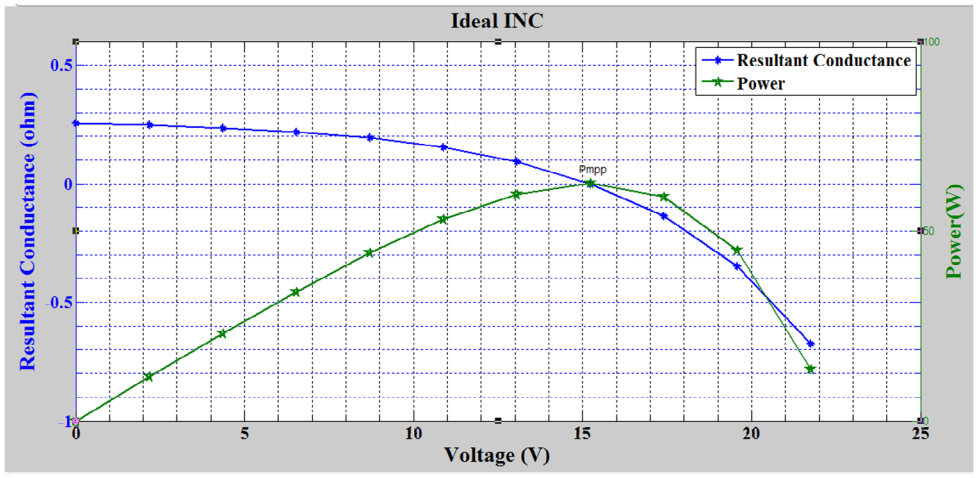

Figure 1. Plot of resultant conductance and power against voltage for an ideal maximum power point tracking technique.

Figure 1 shows the plot of power and resultant conductance against voltage at MPP. Figure 1 shows that power is at its maximum when the resultant conductance (Υ) is zero and it occurs at V_{mpp}. It is also observed from Figure 1 that power at MPP (P_{mpp}) occurs at V_{mpp}. Any MPPT technique with resultant conductance equals to zero at V_{mpp} and maximum power at V_{mpp} is an ideal maximum point tracking technique. Ideally, maximum power occurs when the resultant conductance is equal to zero.

$$\Upsilon = \frac{dI}{dv} + \frac{I}{v} \tag{1}$$

The objective of this paper is to develop an optimized adaptive differential conductance technique that will accurately track the MPP. This technique was developed to solve the problem of conventional INC technique such as tracking accuracy.

The difference between optimized adaptive differential conductance technique and the conventional incremental technique is the replacement of $\frac{I}{V}$ with $\frac{I_{mpp}}{V_{mpp}}$. In this paper, $\frac{I}{V}$ as replaced with $\frac{I_{mpp}}{V_{mpp}}$ to ensure that MPP is tracked with better accuracy.

2. Derivation of optimized adaptive differential conductance technique

Optimized adaptive differential conductance technique is a modified INC technique that is developed using a single diode model of the solar cells. A single diode model is given in Figure 2. The circuit consists of the series resistor (R_s) and a shunt resistor (R_{sh}). A large value of series resistor leads to the large voltage drop across it and this leads to drop in terminal voltage for the same current. Series resistance losses are most important at high illumination intensities (Mahapatro, 2013). R_{sh} are added to the circuit which limits the performance of the cell and also accounts for the dissipative phenomena at the cell internal losses. This implies that very high value of R_{sh} leads to significant reduction in short circuit current. The parallel resistance takes care of the recombination losses,

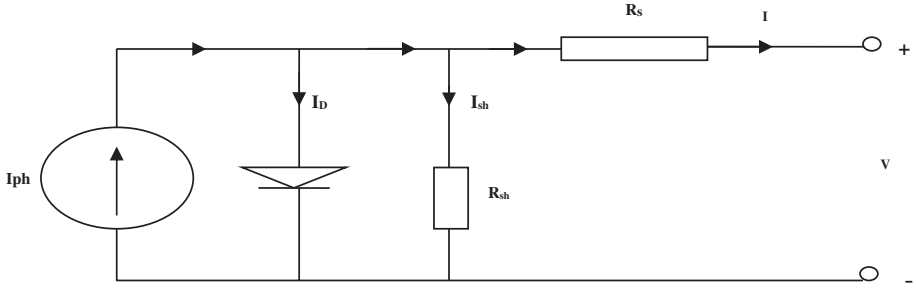

Figure 2. The equivalent circuit of PV cell with single diode.

Source: Adamo, Attivissimo, Di Nisio, Lanzolla, and Spadavecchia (2009).

mainly due to thickness, surface effect and the non-ideality of the junction. The circuit also consists of the photovoltaic currents (I_{ph}), the diode current (I_D) and shunt current (I_{sh}). The value of R_s and R_{sh} modifies shunt circuit current of the cell in a single diode equivalent circuit of PV, Photo generated I_{ph} and the following equivalent electrical circuit results as in Figure 2.

Applying Kirchhoff's law to the nodes of the circuit of Figure 2 yields (3) (Al-hamadi, 2014).

$$I = I_{ph} - I_D - I_{sh} \tag{3}$$

where, I = Output current (load current), I_{ph} = Photo generated current, I_D = Diode current and I_{sh} = Shunt current

For all environmental conditions, current generated by the photovoltaic cell I_{ph} is expressed by (4) (Chouder, Silvestre, Sadaoui, & Rahmani, 2012).

$$I_{ph} = I_{sc}\left[1 + k_i(T - T_{\text{ref}})\right]\frac{G}{G_{\text{ref}}} \tag{4}$$

where, I_{sc} = Short circuit current (A), K_i = Shunt circuit current temperature coefficient of the cell (/°C), T and T_{ref} are the working temperatures of the cell and the reference temperature of the cell respectively in Kelvin, and G and G_{ref} are the solar radiation on the cell surface and reference solar radiation respectively in W/m^2.

However, at STC, Equation (4) becomes $I_{ph} = I_{sc}$.

The current passing through the diode (I_D) in this type of system is given by (5).

$$I_D = I_0\left(\text{Exp}\left(\frac{qV}{AnkT} - 1\right)\right) \tag{5}$$

where, q = Electron charge (1.602×110^{-19}C), k = Boltzmann's constant (1.3865×10^{-23} J/K), T = Cell temperature in Kelvin, A = Diode ideality constant (A = 2 for Silicon, 1 for Germanium), n = Number of PV cells in series, and I_o = Reverse saturation current of the diode and is given by (6)

$$I_0 = I_{rs}\left[\frac{T}{T_{\text{ref}}}\right]^3 \text{Exp}\left[\left(\frac{qE_{\text{gap}}}{Ak}\right)\left(\frac{1}{T_{\text{ref}}} - \frac{1}{T}\right)\right] \tag{6}$$

where, E_{gap} = Energy band gap of the semiconductor material (Andalibi, Rostami, & Darvish, 2016; Bellia, Youcef, & Fatima, 2014), and I_{rs} = Diode saturation current and it is given by (7)

$$I_{rs} = \frac{I_{sc}}{\left[\text{Exp}\left(\frac{qV_{oc}}{AkT} - 1\right)\right]} \tag{7}$$

where I_{sc} and V_{oc} are the short circuit current and open circuit voltage respectively.

I_{sh} is the saturation current through the shunt resistance and using current division rule it becomes

$$I_{sh} = \frac{V_D}{R_{sh}} = \frac{V + IR_s}{R_{sh}} \tag{8}$$

Substituting (5) and (8) into (3), then (3) yields Equation (9)

$$I = I_{ph} - I_0\left(\text{Exp}\frac{q(V + IR_s)}{AnkT} - 1\right) - \frac{V + IR_s}{R_{sh}} \tag{9}$$

Equation (9) is a general I-V characteristic equation of PV cell based on single diode model (Kumar, Shaktawat, Kumar, & Lal, 2013).

2.1. Assumption and approximations of some parameters made in this work

In this research work, Equations (10) to (19) are general equations that lead to successful development of the model. Equations (20), (21) and (23) are the models developed in this paper. They are used for calculating the voltage at the MPP, current at MPP and optimized adaptive differential conductance respectively.

Case 1: Using a single diode model, for *n*-cell PV with R_{sh} very large and R_s very small, I_{sh} will tend to zero and therefore (4) can be rewritten as in (10) (Abd, Wooi, & Selvaraj, 2013; Visweswara, 2013).

$$I = I_{ph} - I_0\left(\text{Exp}\frac{q(V+IR_s)}{AnkT} - 1\right) - 0 \tag{10}$$

Equation (10) can be further simplified as shown in (11).

$$I = I_{ph} - I_0\left(\text{Exp}\frac{q(V+IR_s)}{AnkT}\right) \tag{11}$$

Case 2: At open circuit, I = zero and $V = V_{oc}$, therefore (11) becomes (12) (Kumar et al., 2013).

$$I_{ph} = I_0\left[\text{Exp}\left(\frac{qV_{oc}}{AnkT}\right)\right] \tag{12}$$

Substituting (4) in (12), the open circuit voltage (V_{oc}) is rewritten as (13).

$$V_{oc} = \frac{AnkT}{q}\left(\log_e\left[\frac{I_{sc}\left[1+k_i(T-T_{\text{ref}})\right]\frac{G}{G_{\text{ref}}}}{I_0}\right]\right) \tag{13}$$

Case 3: At short circuit current $V = 0$ and I_{sc} will be written as in (16) (Mahapatro, 2013). Equation (14) can be rewritten as in (15).

$$I_0\left(\text{Exp}\frac{qI_{sc}R_s}{AnkT}\right) = \left[I_0 + \frac{1}{1000}\right] \tag{14}$$

$$\text{Exp}\frac{qI_{sc}R_s}{AnkT} = 1 + \frac{1}{1000} \tag{15}$$

To obtain the short circuit current of a single diode model, Equation (15) can be rewritten as in (16). Substituting (16) and (4) in (11), the load current of the PV cell is given as in (17).

$$I_{sc} = \frac{AnkT}{qR_s}\log_e\left(1 + \frac{1}{1000I_0}\right) \tag{16}$$

The power delivered to the load by the PV system is given by (18). Substituting (17) in (18) and differentiating with respect to V gives (19).

$$P = VI \tag{18}$$

where the input parameter V is such that $0 \leq V \leq V_{oc}$

$$\frac{dp}{dv} = \left(\frac{AnkT}{qR_s}\log_e\left(1+\frac{1}{1000I_0}\right)\left[1+k_i\left(T-T_{ref}\right)\right]\frac{G}{G_{ref}}\right) - I_0\text{Exp}\left(\frac{qV}{AnkT}\right)\left[\frac{qV}{AnkT}+1\right] \quad (19)$$

At MPP $\frac{dp}{dv} = 0$. Solving Equation (19) for V at MPP, Equation (20) is obtained.

$$V_{mpp} = \frac{AnkT}{q}\left[\log_e\left(\frac{\frac{AnkT}{qR_s}\log_e\left(1+\frac{1}{1000I_0}\right)\left[1+K_i\left(T-T_{ref}\right)\right]\frac{G}{G_{ref}}}{I_0}\right) - \log_e\left(1+\frac{qV}{AnkT}\right)\right] \quad (20)$$

To determine the current of the PV cell at MPP (I_{mpp}), (20) is substituted in (11) and (21) is obtained.

$$I_{mpp} = \left(\frac{AnkT}{qR_s}\log_e\left(1+\frac{1}{1000I_0}\right)\left[1+k_i\left(T-T_{ref}\right)\right]\frac{G}{G_{ref}}\right) - I_0\left[\text{Exp}\left(\frac{qV_{mpp}}{AnkT}\right)\right] \quad (21)$$

Equation (20) and (21) represents the voltage and current at MPP of a PV panel respectively.

To determine the ratio of output current to the output voltage of the PV cell, differentiate (11) with respect to cell output voltage and Equation (22) is obtained.

$$\frac{dI}{dV} = \frac{qI_0}{AnkT}\text{Exp}\left(\frac{qV}{AnkT}\right) \quad (22)$$

But the resultant conductance of the system is given by (23) where Υ is the resultant conductance (in mho) and $\frac{dI}{dV}$ the slope in A/V.

$$\Upsilon = \left(\frac{I_{mpp}}{V_{mpp}} - \frac{dI}{dV}\right) \quad (23)$$

When (20), (21) and (22) are substituted in (23), Equation (24) is obtained.

$$\Upsilon = \left(\frac{\left(\frac{AnkT}{qR_s}\log_e\left(1+\frac{1}{1000I_0}\right)\left[1+K_i\left(T-T_{ref}\right)\right]\frac{G}{G_{ref}}\right) - I_0\left[\exp\left(\frac{qV_{mpp}}{AnkT}\right)\right]}{V_{mpp}} - \frac{qI_0}{AnkT}\text{Exp}\left(\frac{Vq}{AnkT}\right)\right) \quad (24)$$

Equation (24) is the model developed in this paper. This model can be compared with the conventional INC model represented in (2). This technique differs from the conventional INC technique as it considered $\frac{I_{mpp}}{V_{mpp}}$ instead of $\frac{I}{V}$ and this leads to better accuracy.

From (24), the conductance of the PV panel $\left(\frac{1}{Z_{panel}}\right)$ and conductance of the load $\left(\frac{1}{Z_{load}}\right)$ are represented as in (25) and (26) respectively.

$$\frac{1}{Z_{panel}} = \frac{\left(\frac{AnkT}{qR_s}\log_e\left(1+\frac{1}{1000I_0}\right)\left[1+k_i\left(T-T_{ref}\right)\right]\frac{G}{G_{ref}}\right) - I_0\left[\text{Exp}\left(\frac{qV_{mpp}}{AnkT}\right)\right]}{V_{mpp}} \quad (25)$$

$$\frac{1}{Z_{load}} = \frac{I_0 q}{AnkT}\text{Exp}\left(\frac{Vq}{AnkT}\right) \quad (26)$$

For maximum power transfer to be achieved, Υ must be equal to zero and therefore, $\frac{1}{Z_{panel}} = \frac{1}{Z_{load}}$..

This technique achieves this by balancing the impendence of the photovoltaic panel with that of the

Table 1. The input and output parameters

Input data			Output data	
Names of parameter	**Symbol**	**Value**	**Names of parameter**	**Symbol**
Reverse saturation current	I_0	0.07 A	Output power	P
Series resistance	R_s	0.008 Ω	Open circuit voltage	V_{oc}
Diode ideality factor	A	2	Short circuit current	I_{sc}
Number of cells	n	100	Output current	I
Electron charge	Q	1.6×10^{-19}°C	Resultant conductance	Υ
Boltzmann's constant	k	1.3805×10^{-23} J/K	Current maximum power point	I_{mpp}
Reference temperature	T_{ref}	298 K	Load conductance (slope)	$\frac{dI}{dV}$
Working temperatures	T	298, 328, 358 K	Voltage maximum power point	V_{mpp}
Reference irradiance	G_{ref}	1,000 W/m^2	Photovoltaic current	I_{ph}
Working irradiance	G	1,000, 800, 600 W/m^2	Panel conductance	$\frac{I_{mpp}}{V_{mpp}}$
Voltage	V	$0–V_{oc}$		

load. Comparing Equation (2) and (23), it is observed that (2) differentiated only the voltage and current but (23) differentiated the voltage and current at MPP which will give accurate MPP.

2.2. Performance metrics

Performance metrics are measurement standard that is used to evaluate the performance of models. Ideal MPPT Accuracy (IMTA) will be used to evaluate the effectiveness of the proposed model. This is obtained by taking the absolute difference of the average mean of new and old techniques, dividing it by the old technique and taking the percentage as shown in Equation (27) where N is the number of data points.

$$\text{IMTA} = \frac{\frac{1}{N}\left|\sum \Upsilon_{\text{old}}\right| - \frac{1}{N}\left|\sum \Upsilon_{\text{new}}\right|}{\frac{1}{N}\left|\sum \Upsilon_{\text{old}}\right|} \times 100 \tag{27}$$

The performance of proposed model was validated using conventional incremental conductance. The conventional incremental conductance technique is selected because it has good performance, low cost and easy to implement (Safari & Mekhilef, 2011).

2.3. Parameters and definitions

The input and output parameters used in the model development are explained as shown in Table 1.

3. Results and discussion

The data obtained from the Equations (2), (18) and (24) were shown in Tables 2–5. Considering Table 2, results showed how resultant conductance and output power of PV system varies with PV voltage at STC. From table, it was observed that the power output increased with increase in voltage (V) for $V \leq V_{mpp}$ and decreased with increase in V for $V > V_{mpp}$. On the other hand, the resultant conductance varied inversely as V for $0 \leq V \leq V_{oc.}$ For $V \leq V_{mpp}$, the resultant conductance is positive and this implies that the model is forwardly tracking the MPP. For $V > V_{mpp,}$ the resultant conductance is negative and this implies that the model is backwardly tracking MPP.

The relationship in Table 2 was clearly shown in Figure 3. From Figure 3, resultant conductance is positive and it varies inversely with voltage for $V \leq V_{mpp}$. On the other hand, as the power is increasing, the voltage is also increasing for $V \leq V_{mpp}$. From the point that V_{mpp} is attained, the power started varying inversely with the voltage. However, the resultant conductance continues to be inversely proportional to the voltage, though, it is negative in this region. The change in sign of the resultant conductance about the MPP makes the model adaptive in tracking MPP.

Table 2. The resultant conductance (ϒ) and power varies with voltage at 1,000 W/m² and 298 K (STC) for the proposed model

Data point	ϒ (mho)	Power (W)	Voltage (V)
1	0.3903	0	0
2	0.3832	19.5811	2.1758
3	0.3722	38.9168	4.3516
4	0.3554	57.8128	6.5274
5	0.3298	75.9383	8.7032
6	0.2906	92.7358	10.879
7	0.2308	107.274	13.0548
8	0.1395	118.009	15.2306
9	**-8.3243×10^{-6}**	**122.395**	**17.4064**
10	−0.2131	116.262	19.5822
11	−0.5386	92.8034	21.758
12	−1.0359	40.9619	23.9338

Table 3. The resultant conductance (ϒ) varies with voltage at varying Solar irradiance and temperature of 298 K for the proposed model

600 W/m²	800 W/m²	1,000 W/m²	Voltage (V)
Resultant conductance			
ϒ (mho)	ϒ (mho)	ϒ (mho)	
0.2539	0.3235	0.3903	0.0000
0.2467	0.3163	0.3832	2.1758
0.2357	0.3053	0.3722	4.3516
0.2189	0.2885	0.3554	6.5274
0.1933	0.2629	0.3298	8.7032
0.1542	0.2237	0.2906	10.879
0.0944	0.1639	0.2308	13.0548
0.003	0.0726	0.1395	15.2306
−0.1365	−0.0669	-8.3243×10^{-6}	17.4064
−0.3496	−0.28	−0.2131	19.5822
−0.6751	−0.6055	−0.5386	21.7580

Table 3 showed how resultant conductance and power varies with the voltage at different irradiance. It was observed from table that the resultant conductance was directly proportional to the received irradiance for all values of the input voltage. The results showed that the higher the value of irradiance, the higher the value of resultant conductance. This is because the impedance of panel falls with the increase in irradiance while the impedance of the load is constant. The relationship in Table 3 was clearly shown in Figure 4.

Figure 4 showed the resultant conductance-voltage relationship at 298 K and 600, 800 and 1,000 W/m². From figure, it was observed that the resultant conductance increases as the irradiance increases and vice versa. This is because the impedance of the panel decreased as the irradiance is increasing while the impedance of the load is not affected by the irradiance. This showed that matching of panel impedance with load impedance using this model is faster at low irradiance but less accurate.

Figure 3. Plot of resultant conductance and power against voltage for the proposed model.

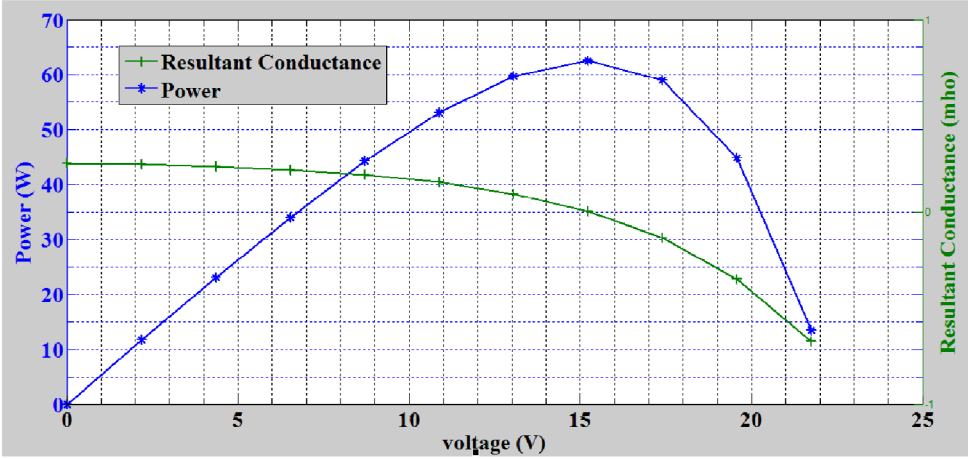

Figure 4. Plot of resultant conductance against voltage at different irradiance for the proposed model.

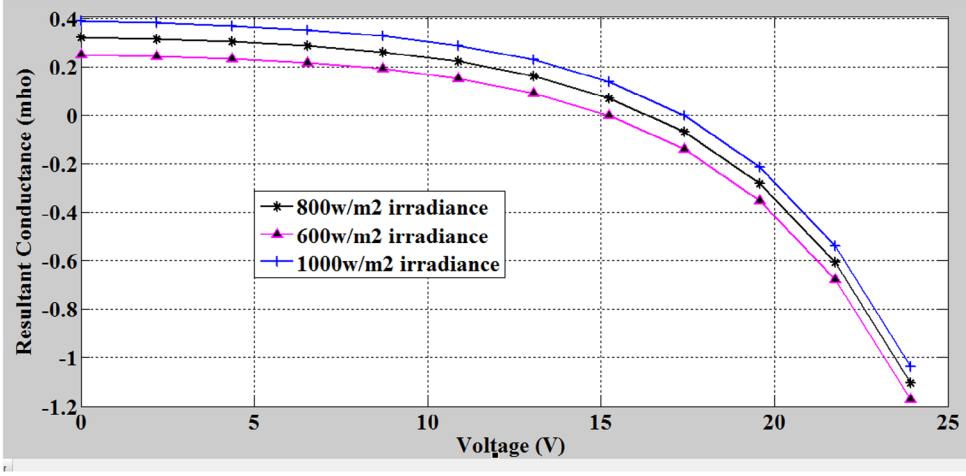

Table 4. Variation of resultant conductance with voltage at 1,000 W/m² irradiance for varying temperatures for the proposed model

298 K	328 K	358 K	Voltage (V)
Resultant conductance			
ϒ (mho)	ϒ (mho)	ϒ (mho)	
0.3903	0.3403	0.2909	0.0000
0.3832	0.3345	0.2861	2.1758
0.3722	0.3259	0.2793	4.3516
0.3554	0.3134	0.2696	6.5274
0.3298	0.2949	0.2557	8.7032
0.2906	0.2678	0.2361	10.8790
0.2308	0.2280	0.2081	13.0548
0.1395	0.1694	0.1683	15.2306
−8.3243 x 10^{-6}	0.0834	0.1117	17.4064
−0.2131	−0.0429	0.0311	19.5822
−0.5386	−0.2286	−0.0835	21.7580
−1.0359	−0.5015	−0.2466	23.9338

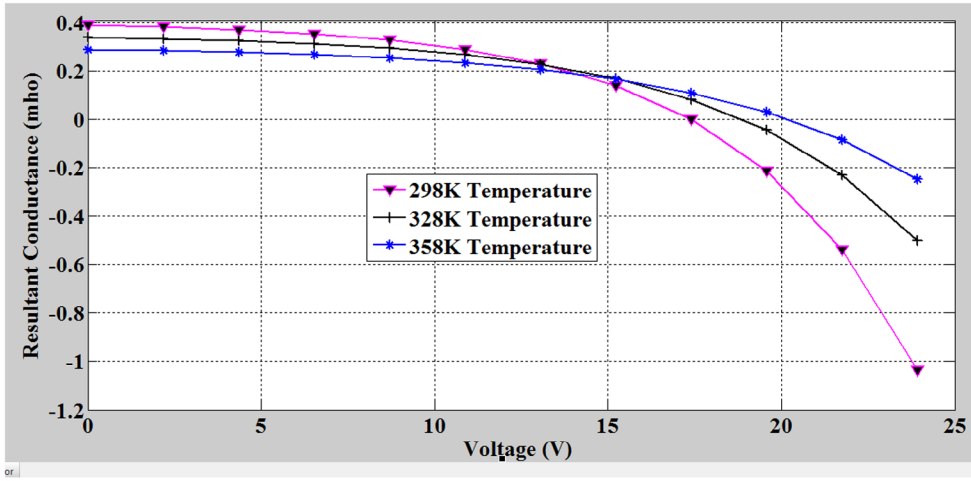

Figure 5. Plot of resultant conductance against voltage at different temperature for the proposed model.

Table 4 showed how the resultant conductance varies with the voltage at 1,000 W/m² irradiance at 298, 328 and 358 K. From table, it was observed that resultant conductance varied inversely with the temperature for $V \leq V_{mpp}$. However, for $V > V_{mpp}$, the resultant conductance is directly proportional to the temperature. This is because panel impedance decreases with the increase in panel temperature (this behaviour is right since the panel is made from semiconductor) and panel temperature has no effect on the load impedance. Table 4 also showed that the model tracks MPP faster and more accurately at low temperature. The relationship in Table 4 was clearly shown in Figure 5.

Figure 5 showed how the resultant conductance varies with voltage for temperatures of 289, 328 and 358 K. The characteristic behaviour in Figure 5 showed that the resultant conductance was inversely proportional to the temperature of the PV panel for $V \leq V_{mpp}$ and directly proportional to the temperature for $V > V_{mpp}$. Figure also showed that the model tracks MPP faster and more accurately at low temperature.

Table 5. Variation of resultant conductance with voltage at 600 w/m² and 298 k for the proposed model and conventional incremental conductance technique

Data point	Optimized adaptive differential conductance (OADC) at 600 W/m²	Conventional incremental conductance at 600 W/m²	Powers at 600 W/m²	Voltage (V)
	Resultant conductance			
	ϒ (mho)	ϒ (mho)	P (W)	
1	0.2539	0.2090	0.0000	0.0000
2	0.2467	0.2018	11.6556	2.1758
3	0.2357	0.1909	23.0658	4.3516
4	0.2189	0.1741	34.0363	6.5274
5	0.1933	0.1485	44.2363	8.7032
6	0.1542	0.1093	53.1083	10.8790
7	0.0944	0.0495	59.7210	13.0548
8	**0.0030**	**−0.0418**	**62.5302**	**15.2306**
9	−0.1365	−0.1813	58.9910	17.4064
10	−0.3496	−0.3944	44.9322	19.5822
11	−0.6751	−0.7199	13.5483	21.7580

Figure 6. Plot of resultant conductance and power against voltage.

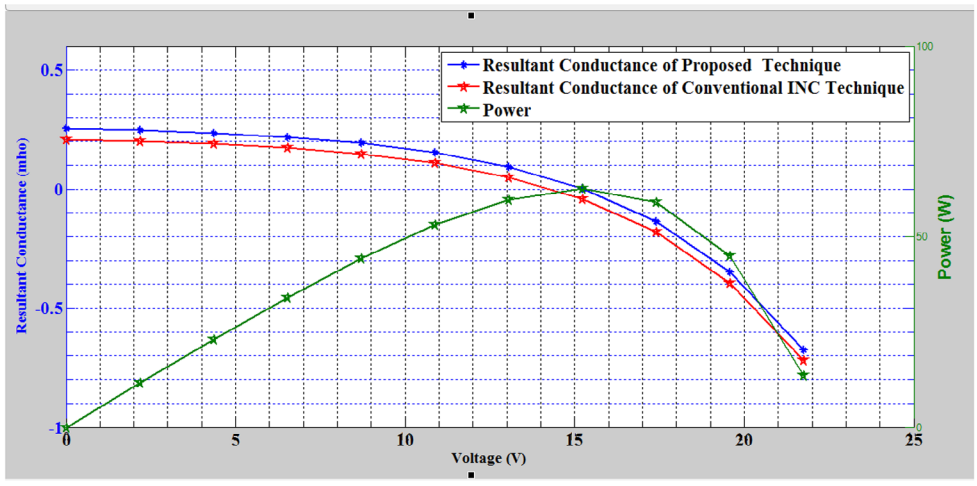

Table 5 showed how the resultant conductance varies with the voltage at 600 W/m^2 and 298 K for the proposed and conventional INC technique. From table, it was observed that at 600 W/m^2 and 298 K, the resultant conductance of optimized adaptive differential conductance was larger than the resultant conductance of conventional INC technique. It was also observed that at V_{mpp}, the resultant conductance of the proposed technique is closer to the value for the ideal model (zero) compared to the resultant conductance of the INC technique. Using Equation (27), it was observed that the proposed model has accuracy improvement of 6.0558% over the conventional INC technique. However, the speed of tracking the MPP is the same for both models. This is because the MPP occurs at data point eight for the two models.

The results in Table 5 were clearly presented in Figure 6. From figure, it was observed that the plot of the resultant conductance of the proposed technique against voltage intersected the plot of power against the voltage at the V_{mpp} while that of the INC technique intersected the power plot at a point far from V_{mpp}. This also showed that the developed technique has better accuracy. However, the data point plots of each model correspond showing that the two models have the same speed (Table 6).

Table 6. Symbols and its nomenclatures

Symbol	Nomenclature	
	Lowercase	**Uppercase**
A		alpha
N		nu
Q		qu
k		kappa
P		rho
V	Nu	
T		tau
I		lota
ϒ	Gamma	

5. Conclusion

In this paper, optimized adaptive differential conductance technique was successfully developed.

The model developed was simulated using MATLAB. From the result, it was observed that the new model was very accurate. It tracks the MPP faster and more accurately at low temperature. On the other hand, the MPP is tracked faster at low irradiance but the tracking is more accurate at higher irradiance. In comparison with conventional INC technique, it was noticed that the optimized adaptive differential conductance technique developed was 6.0558% more accurate. The importance of the result obtained in this research is that it showed the expected performance of the techniques developed. The result will act as a lookup table and chart for designers as it concerns some input and expected out parameters. The significance of the method developed in this paper is that it will lead to the implementation of better MPPT-based charge controller for photovoltaic application. Charge controller developed using this method will maximize the transfer of power from the PV panel to the load with minimal loss.

Author details
Val Hyginus U. Eze[1]
E-mail: ezehyginusudoka@gmail.com
Ogechukwu N. Iloanusi[1]
E-mail: ogechukwu.iloanusi@unn.edu.ng
Martin C. Eze[1]
E-mail: martin.eze@unn.edu.ng
Charles C. Osuagwu[1]
E-mail: charles.osuagwu@unn.edu.ng
[1] Electronic Engineering, University of Nigeria, Nsukka, Nigeria.

Citation information
Cite this article as: Maximum power point tracking technique based on optimized adaptive differential conductance, Val Hyginus U. Eze, Ogechukwu N. Iloanusi, Martin C. Eze & Charles C. Osuagwu, *Cogent Engineering* (2017), 4: 1339336.

References

Abd, N., Wooi, H., & Selvaraj, J. (2013). Photovoltaic module modeling using simulink/matlab. In *The 3 rd International Conference on Sustainable Future for Human Security* (Vol. 17, pp. 537–546). Elsevier B.V. doi:10.1016/j.proenv.2013.02.069

Adamo, F., Attivissimo, F., Di Nisio, A., Lanzolla, A. M. L., & Spadavecchia, M. (2009). Parameters estimation for a model of photovoltaic panels. In *19th IMEKO world congress on fundamental and applied metrology* (pp. 964–967). Libson, portugal.

Al-hamadi, H. (2014). Estimation of photovoltaic cell parameters using piecewise linear approximation. *International Journal of Computer Science and Electronics Engineering, 2*, 28–30.

Andalibi, S., Rostami, A., & Darvish, G. (2016). Band gap engineering of organo metal lead halide perovskite photovoltaic absorber. *Optical and Quantum Electronics*. doi:10.1007/s11082-016-0525-y

Azimi, S., Dehkordi, B. M., & Niroomand, M. (2012). An adaptive incremental conductance MPPT based on BELBIC controller in photovoltaic systems. In *20th Iranian Conference on Electrical Engineering, 4*, 324–329.

Bellia, H., Youcef, R., & Fatima, M. (2014). A detailed modeling of photovoltaic module using MATLAB. *NRIAG Journal of Astronomy and Geophysics, 3*, 53–61. doi:10.1016/j.nrjag.2014.04.001

Chafle, S. R., & Vaidya, U. B. (2013). Incremental conductance MPPT technique FOR PV system. *International Journal of Advanced Research in Electrical, Electronics and Instrumentation Engineering, 2*, 2719–2727.

Chouder, A., Silvestre, S., Sadaoui, N., & Rahmani, L. (2012). Modeling and simulation of a grid connected PV system based on the evaluation of main PV module parameters. *Simulation Modelling Practice and Theory, 20*, 46–58. doi:10.1016/j.simpat.2011.08.011

Eze, M. C., & Olisa, S. C. (2015). Performance characterization of building integrated photovoltaic systems in northern and southern hemisphere locations. *International Journal of Engineering Science, 6*, 1606–1613.

Kumar, S., Shaktawat, K. S., Kumar, P., & Lal, A. K. (2013). A typical assessment of photovoltaic array: Modelling, simulation and application aspects. *International Journal of Engineering Trends and Technology, 4*, 1407–1410.

Mahapatro, S. K. (2013). Maximum power point tracking (MPPT) Of solar cell using buck-boost converter. *International Journal of Engineering & Technology, 2*, 1810–1821.

Nguyen, T. L., Low, K., & Member, S. (2010). A global maximum power point tracking scheme employing DIRECT search algorithm for photovoltaic systems. *IEEE Transactions on Industrial Electronics, 57*, 3456–3467. https://doi.org/10.1109/TIE.2009.2039450

Safari, A., & Mekhilef, S. (2011). Incremental conductance MPPT method for PV systems. In *Canadian Conference on Electrical and Computer Engineering* (pp. 000345–000347). doi: 10.1109/CCECE.2011.6030470

Topic, M., Brecl, K., Kurnik, J., & Sites, J. (2006, September). Effective efficiency and performance ratio as energy rating system for PV modules. In *21st European conference on Photovoltaic Solar Energy*, 2507–2510.

Visweswara, K. (2013). An Investigation Of Incremental Conductance Based Maximum Power Point Tracking For Photovoltaic System. In *4th International Conference on Advances in Energy Research* (Vol. 54, pp. 11–20). Elsevier B. V. doi:10.1016/j.egypro.2014.07.245

© 2017 The Author(s). This open access article is distributed under a Creative Commons Attribution (CC-BY) 4.0 license.

You are free to:
Share — copy and redistribute the material in any medium or format
Adapt — remix, transform, and build upon the material for any purpose, even commercially.
The licensor cannot revoke these freedoms as long as you follow the license terms.

Under the following terms:
Attribution — You must give appropriate credit, provide a link to the license, and indicate if changes were made.
You may do so in any reasonable manner, but not in any way that suggests the licensor endorses you or your use.
No additional restrictions

You may not apply legal terms or technological measures that legally restrict others from doing anything the license permits.

Cogent Engineering **(ISSN: 2331-1916) is published by Cogent OA, part of Taylor & Francis Group.**

Publishing with Cogent OA ensures:

- Immediate, universal access to your article on publication
- High visibility and discoverability via the Cogent OA website as well as Taylor & Francis Online
- Download and citation statistics for your article
- Rapid online publication
- Input from, and dialog with, expert editors and editorial boards
- Retention of full copyright of your article
- Guaranteed legacy preservation of your article
- Discounts and waivers for authors in developing regions

Submit your manuscript to a Cogent OA journal at www.CogentOA.com